



## DISLOCATION NUCLEATION FROM A CRACK TIP: A FORMULATION BASED ON ANISOTROPIC ELASTICITY

YUEMIN SUN† and GLENN E. BELTZ‡

†Division of Applied Sciences, Harvard University, Cambridge, MA 02138, U.S.A.

‡Department of Mechanical and Environmental Engineering, University of California, Santa Barbara, CA 93106, U.S.A.

(Received 20 January 1994; in revised form 13 August 1994)

### ABSTRACT

The analysis of dislocation emission from a crack tip within the Peierls framework [Rice (1992) *J. Mech. Phys. Solids* **40**, 239–271; Rice *et al.* (1992) *Topics in Fracture and Fatigue*, pp. 1–58; Sun *et al.* (1993) *Mater. Sci. Engng A* **170**, 67–85], heretofore developed for isotropic solids, is generalized to take into account elastic anisotropy. An incipient dislocation core, represented in terms of a critical configuration at the crack tip, is determined numerically (most simply in the shear-only version of the model, but also for a combined tension–shear version that includes tension–shear coupling constrained by atomic modeling). These solutions improve upon approximations based on an effective shear stress intensity. For fcc crystals and intermetallics, the nucleation event analysed is that of a set of partial dislocations emitted sequentially. The anisotropic formulation accounts for corrections as large as 30% in the critical value of the stress intensity factor for atomic decohesion, or cleavage. The anisotropic critical crack extension force for dislocation emission may be greater or less than its isotropic counterpart. For an embedded-atom-method (EAM) model of bcc  $\alpha$ -Fe, the anisotropic values can be as large as 2.4 times the isotropic ones in one crack orientation; in another crack orientation, the values are as much as 40% less than the isotropic analogs. For fcc structures (EAM nickel, aluminum and Ni<sub>3</sub>Al), the difference is within a  $\pm 10$ –25% range. For silicon, the isotropic formulation is good, with less than a 14% difference from the anisotropic counterpart. The anisotropic effects are found to increase with a standard ratio of elastic anisotropy, and are important for predicting intrinsic ductile versus brittle response.

### INTRODUCTION

The recent analysis of dislocation emission from a crack tip by Rice (1992) is based on the Peierls–Nabarro model (Peierls, 1940; Nabarro, 1947) for a straight line dislocation. This model combines atomistic descriptions of the dislocation core with continuum elasticity in a physically realistic fashion and describes the process of a dislocation core nucleated from nil at a crack tip. In the same way as in the Peierls–Nabarro model of a dislocation core, the nucleating incipient dislocation at a crack tip is depicted as follows: a distribution of discontinuity in the displacement field across the slip plane obeys a sinusoidal law of shear stress versus displacement, and is embedded in a linear elastic medium surrounding the crack. The main advantage of the new approach is the elimination of the ill-defined dislocation core cut-off radius  $r_c$ , used in the earlier pioneering work by Rice and Thomson (1974). The newly

identified physical property by Rice (1992), a solid state parameter  $\gamma_{\text{us}}$ , the *unstable stacking energy*, is now the key to the analysis of dislocation emission from a crack tip in the Peierls framework. We note that the newer approach contains no account of the energy of the ledge formed at the crack tip by the emergent dislocation, and it remains to be seen how important that factor is.

Additional reservations should be made here regarding the Peierls-type analysis for dislocation emission. Recent atomistic studies by Zhou *et al.* (1994) indicate that the Peierls model may underestimate the critical loading for dislocation emission by as much as 50% when the slip plane is tilted with respect to the crack plane. The agreement of the two types of approaches is good in the case of coplanar crack and slip planes (Zhou *et al.*, 1993). Whether the discrepancy is due to the discrete nature of the system, so as to result in lattice trapping in the slip process or the so-called ledge effect, remains open for further research. The atomistic simulations of crack tips in RuAl (Becquart *et al.*, 1993) showed that surface reconstructions may be induced under mode I loading on the near-tip crack surfaces, and may determine whether or not the dislocation is emitted. We note that the Peierls model does not take into account stress-induced surface reconstructions, which may alter the predictions by the Peierls model and the Griffith cleavage condition. These issues are generic in nature, and likely are beyond the scope of what the Peierls model can handle.

Furthermore, we note that the embedded-atom-method (EAM) representation of "real" iron is only fair: it does not directly consider magnetic effects, and can only mimic their consequences in fitting the vacancy energy and the requirement that energy of bcc be lower than fcc and hcp structures. The fit to the elastic constants is only fair because of this requirement. Interested readers should consult the original paper (Harrison *et al.*, 1990) for details. However, despite this, it is still appropriate that we compare the predictions of the Peierls type analysis with the observations in molecular dynamics (MD) simulations using the same EAM potential by Cheung and Yip (1990, 1994), Cheung (1990), and Cheung *et al.* (1991).

It has been determined that the tensile stress across a slip plane ahead of a crack tip has the effect of decreasing the critical loading required to emit a dislocation: evaluation of the effect is important for understanding ductile versus brittle response. The details of estimating the tension-shear coupling parameters and a systematic study of coupling effects were carried out by calculating the criteria for dislocation nucleation for a wide range of these parameters, and results were presented in Rice *et al.* (1992), Sun *et al.* (1993), and Sun (1993).

The Peierls concept has also been used in a recent analysis of dislocation nucleation by Schöck (1991). His analysis was somewhat more approximate compared to Rice's (1992) Peierls type analysis and did not uncover the exact critical core configuration of the nucleated dislocation within the Peierls framework. There, a simple *arctan* function was instead assumed for the core and used for variational determination.

Since all crystals are anisotropic and most existing atomistic MD simulations correspond to *anisotropic* crystals, the problem of dislocation emission from a crack tip should be analysed based on the anisotropic elasticity formulation. The objective of this work is to generalize the analysis of dislocation nucleation at a crack tip within the Peierls framework from the previous isotropic elasticity formulation to anisotropic

elasticity. Some preliminary work towards that end, giving shear-only results for coincidental crack and slip planes, was reported by Rice *et al.* (1992).

After a brief description of anisotropic elasticity, dislocation emission from a crack tip is first treated in the approximation of an effective shear stress intensity factor and without tension–shear coupling. The exact numerical solutions improve upon the approximate treatments based on an effective shear stress intensity. The incipient dislocation core and its critical configuration at the crack tip is exactly solved numerically, most simply in the shear-only version of the model, but also for a combined tension–shear version that includes tension–shear coupling constrained by atomic models. This is done for several EAM metals, as well as silicon, with parameters of slip constitutive laws estimated by density functional theory in the local density approximation (Huang *et al.*, 1991; Huang, private communication; Kaxiras and Duesbery, 1993), referred to as DFT-LDA Si, following Rice *et al.* (1992), Sun *et al.* (1993), and Sun (1993). For the fcc crystals and intermetallics, the nucleation event analysed is that of a set of partial dislocations emitted sequentially. Results are compared to those of the isotropic formation.

## CRACK EXTENSION

The energy release rate of a loaded crack tip in an anisotropic medium is

$$G = K_x \Lambda_{x\beta} K_\beta, \quad (1)$$

where  $K_x = (K_1, K_2, K_3) = (K_{II}, K_I, K_{III})$  is the external loading and  $\Lambda_{x\beta}$  is the appropriate matrix for the crack orientation in the anisotropic material. The Einstein summation convention is used in this article, namely, repeated dummy indices indicate summation. The matrix  $\Lambda_{x\beta}$  is real and symmetric and can be represented by the elastic constants in the crack coordinate system, and has, in general, off-diagonal elements [see Stroh (1958), Bilby and Eshelby (1968), Barnett and Asaro (1972) and Suo (1989)]. The elastic constants for the EAM materials for anisotropic calculations are the fitted results by these atomic models, not the experimental values. The elastic constants and EAM functions used in this work have the following sources: Ni are from Foiles *et al.* (1986) and Foiles and Daw (1987); Al, Hoagland *et al.* (1990); Ni<sub>3</sub>Al, Foiles and Daw (1987);  $\alpha$ -Fe, Harrison *et al.* (1990). Those for Si are the experimental values, listed by Hirth and Lothe (1982).

For convenience, capital letters are used to label crack orientations in cubic crystals, which are listed in Table 1. The coordinate system is: the  $x_1$  axis is the crack extension direction,  $x_2$  is normal to the crack plane, and  $x_3$  is along the crack front. For instance, a crack on the (001) plane growing along the [100] direction is labeled as crack *A*, and along the [110] direction as crack *B*.

Equation (1) is used to calculate the critical loading  $K_{IG}$  for crack extension under mode I loading corresponding to the Griffith condition, that is,  $G = 2\gamma_s$ , where  $\gamma_s$  is the surface energy. For crack *A* in EAM-Fe, with  $\gamma_s$  equal to  $1.83 \text{ J m}^{-2}$ ,  $K_{IG}$  is  $0.864 \text{ MPa } \sqrt{\text{m}}$  in the isotropic formulation, but  $0.665 \text{ MPa } \sqrt{\text{m}}$  in the anisotropic formulation, which is 23% less than the isotropic value. For the isotropic calculation,

Table I. *The crack and slip systems*

Lattice	Crack model	$x_1-x_2-x_3$ , crack coord.	Slip system
bcc	<i>A</i>	[010]-[001]-[100]	(1/2) [11 $\bar{1}$ ] (011)
bcc	<i>B</i>	$\bar{1}$ 10]-[001]-[110]	(1/2) [11 $\bar{1}$ ] ( $\bar{1}$ 10)
bcc	<i>C</i>	[011]-[0 $\bar{1}$ 1]-[100]	(1/2) [11 $\bar{1}$ ] (011)
fcc	<i>D</i>	$\bar{1}$ 10]-[001]-[110]	(1/6) [121] ( $\bar{1}\bar{1}$ )
fcc	<i>E</i>	[001]- $\bar{1}$ 10]-[110]	(1/6) [ $\bar{1}$ 12] ( $\bar{1}\bar{1}$ )
fcc	<i>F</i>	[111]-[1 $\bar{1}$ 0]-[11 $\bar{2}$ ]	(1/6) [211] (11 $\bar{1}$ )
fcc	<i>G</i>	[1 $\bar{1}$ 2]- $\bar{1}$ 11]-[110]	(1/6) [ $\bar{1}$ 12] ( $\bar{1}\bar{1}$ )

$\mu = 0.691 \times 10^{11}$  Pa and  $\nu = 0.323$ , which are Voigt averages of the anisotropic elastic constants for EAM-Fe.

According to isotropic elasticity, the Griffith condition under pure mode I loading would be the same for the crack to extend along any direction in a given plane. However, in an anisotropic elastic crystal, the different crack extension directions have different  $\Lambda_{\alpha\beta}$  matrices, and therefore require different critical pure mode I loadings. Even with the same value of  $G$  equal to  $2\gamma_s$  for (001) crack planes in a cubic crystal, a crack growing along [100] (crack *A*) or [110] (crack *B*) would require different amounts of mode I loading for extension. For EAM-Fe, crack *A*,  $K_{IG}$  is 0.665 but for *B* it is 0.778 in units of MPa  $\sqrt{\text{m}}$ , a 15% difference. Since the anisotropic formulation is necessary for determining the condition of crack extension, we may expect it is also important for dislocation emission.

## DERIVATION OF CRITERIA FOR DISLOCATION NUCLEATION WITHIN THE EFFECTIVE SHEAR STRESS INTENSITY FACTOR APPROXIMATION

In this section, we first treat the problem of dislocation emission from a crack tip within the effective shear stress intensity factor  $K_\tau$  approximation (Rice, 1992; Rice *et al.*, 1992). Let us consider the general scenario: suppose that a "soft" slip plane intersects the crack plane and that the intersection line is also the crack front, and that the slip plane makes an angle  $\theta$  with the crack plane. Assume that the crack tip is loaded by  $(K_1, K_2, K_3) = (K_{II}, K_I, K_{III})$ ; the  $K_x$  here are the local and screened stress intensity factors near the crack tip. Assume that the crack does not extend. The stress concentration near the crack tip is relieved by an emergent zone of displacement discontinuity  $\{\delta_r(r), \delta_\theta(r), \delta_z(r)\}$  across the slip plane, i.e. an incipient dislocation. The incipient slip zone is illustrated in Fig. 1.

The edge slip direction is along  $r$ , the normal direction is along  $\theta$  with the unit directional vector  $\mathbf{n}$  and the screw slip direction is along  $z$ . The edge component is  $\delta_r(r) = u_r^+(r) - u_r^-(r)$  and the screw component  $\delta_z(r) = u_z^+(r) - u_z^-(r)$ ; the discontinuity in the opening direction  $\delta_\theta(r) = u_\theta^-(r) - u_\theta^+(r) = n_x[u_x^+(r) - u_x^-(r)]$ . The slip direction in the slip plane has the unit directional vector denoted  $\mathbf{s} = (\cos \phi, 0, \sin \phi)$  in the  $r, \theta, z$  coordinate system. The sign convention for the angle  $\phi$  of the slip direction is that  $\phi$  is defined as positive when the slip direction rotates from the  $r$  axis

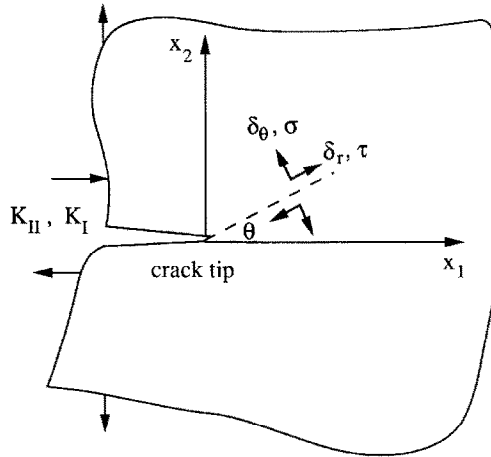


Fig. 1. An incipient dislocation, represented by a distribution of sliding and opening displacements, develops along a tilted slip plane at angle  $\theta$  with respect to the crack plane in response to the mixed loading  $K_{II}$  and  $K_I$ .

toward the  $z$  axis. The displacement discontinuity across the slip plane in that direction is  $\delta_s(r) = s_z \delta_z(r) = s_z [u_z^+(r) - u_z^-(r)]$ .

The lattice restoring stresses at one point  $r$  in the slip plane are assumed to be only a function of the local displacement discontinuity  $\delta_s(r)$  in the slip direction  $s$ . Afterwards only the slip on that direction is considered, namely,  $[\delta_s(r), \delta_z(r)] = [\cos \phi, \sin \phi] \delta_s(r)$ . We present the details for the constrained path approximation later. The modeling of such lattice restoration against shear slip, in a way that also involves opening, has been presented in Sun *et al.* (1993) and Sun (1993), with empirical interatomic potentials in the EAM and with reference to DFT-LDA studies by others (Huang *et al.*, 1991; Huang, private communication; Kaxiras and Duesbery, 1993).

We first analyse the case of coincidental slip and crack planes, i.e.  $\theta = 0$ , and derive the nucleation criterion. There the mathematics simplifies, and an exact analytical solution is possible via the  $J$ -integral method in the shear-only model. The case of an inclined slip plane is approximately treated based on the effective stress intensity factor. Though such an approximate method tends to overestimate the critical loading for dislocation emission, it establishes a conceptual framework. In the next section, we present exact numerical solutions and also treat tension-shear coupling.

*Analysis of coincident crack and slip planes for general loading and Burgers vector angle*

We follow the derivation in Rice (1992), using the  $J$ -integral argument, but instead using anisotropic elasticity, which was partially outlined in Rice *et al.* (1992). The path independent  $J$ -integral is

$$J = \int_{\Gamma} [n_1 W(\nabla \mathbf{u}) - n_\alpha \sigma_{\alpha\beta} \partial u_\beta / \partial x_1] ds, \tag{2}$$

where  $W$  is the strain energy density,  $\sigma_{\alpha\beta}$  is the stress tensor,  $\mathbf{u}$  is the displacement

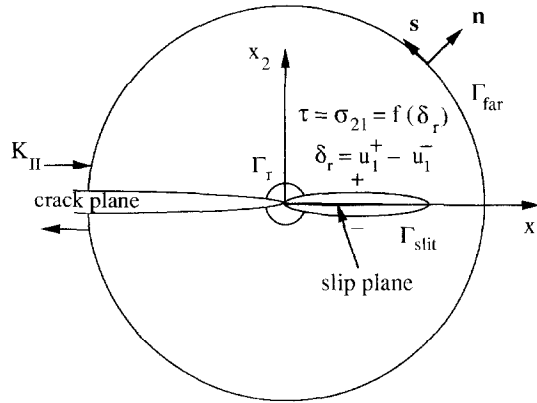


Fig. 2. A semi-infinite crack tip is loaded by  $K_{II}$ , while an incipient shear zone of edge character on the coplanar plane with the crack relieves the singular shear stress field.  $J$ -Integrals are evaluated along the far and slit paths.

field,  $\mathbf{n}$  is the unit normal vector pointing outward from the path  $\Gamma$ , and  $s$  is the arc length. The integral path starts from any traction-free point on the lower crack surface, surrounds the crack tip, and ends on any traction-free point on the upper crack surface. The  $J$ -integral is path independent as long as the elastic properties are independent of  $x_1$  and the equilibrium condition is satisfied.

Figure 2 shows the  $J$ -integral paths around the crack tip. Suppose the incipient slip zone is small compared to the overall size of the crack and specimen, so that we can treat the crack as embedded in an infinite medium and the stress near the tip is dominated by the singular field prescribed by  $K_2$ . This is verified by the numerical solutions to be presented in the next section, since the incipient zone is appreciable over the length of eight or less units of  $b$  ahead of the crack tip. The crack is treated as semi-infinite and the concept of small scale yielding is valid. It is a well known result that evaluation of the  $J$ -integral along the path  $\Gamma_{far}$  which is far from the shear zone but still is small compared to crack length yields  $J = G$ , i.e.

$$J = G = K_2 \Lambda_{2\beta} K_\beta. \tag{3}$$

The emergent slip zone relaxes the singular stress field near the tip. If the stress relief is not complete, there would be some remnant singular stress components, which are describable by the stress intensity factor at the tip  $K_{z(tip)} = [K_{1(tip)}, K_{2(tip)}, K_{3(tip)}]$ . Evaluating the  $J$ -integral along a path closely embracing the slit thus yields two parts: the first arises from integration on a circular path  $\Gamma_r$  with an ever-shrinking radius around the crack tip, resulting from the crack tip singularity, and the second from integration over  $\Gamma_{slit}$ ,

$$J = K_{z(tip)} \Lambda_{z\beta} K_\beta + \int_0^z [-\sigma_{2z} \hat{c} \delta_\beta / \hat{c} x_1] dx_1, \tag{4}$$

where  $\sigma_{2z}$  is the stress across the slip plane for which we assume there exists a potential  $\Phi(\delta)$  such that

$$\sigma_{2\beta} = \partial\Phi(\boldsymbol{\delta})/\partial\delta_\beta, \quad (5)$$

and is related to the  $\delta_\beta$ . The integration of the second term in (4) is easily carried out. The integral is identical to  $\Phi(\boldsymbol{\delta}_{(\text{tip})})$ , an elegant result in that it depends only on the displacement discontinuity at the tip. Therefore,  $J$  evaluated along  $\Gamma_{\text{slit}}$  is

$$J = K_{x(\text{tip})}\Lambda_{z\beta}K_{\beta(\text{tip})} + \Phi(\boldsymbol{\delta}_{(\text{tip})}). \quad (6)$$

Combining (3) and (6) relates the  $K_x$  to the potential  $\Phi(\boldsymbol{\delta}_{(\text{tip})})$ ,

$$K_x\Lambda_{z\beta}K_\beta - K_{x(\text{tip})}\Lambda_{z\beta}K_{\beta(\text{tip})} = \Phi(\boldsymbol{\delta}_{(\text{tip})}). \quad (7)$$

From (7), we obtain information about the slip displacement  $\delta_{x(\text{tip})}$  at the tip via the lattice potential  $\Phi(\boldsymbol{\delta}_{(\text{tip})})$  if we know how the  $K_{x(\text{tip})}$  is determined by the shear zone process under loading  $K_x$ .

As a simplification, we treat the slip process zone  $\{\delta_x(r)\}$  as a pure shear process, i.e. the dilational opening does not enter directly into the formulation of the mechanics problem, which means putting constraints on the opening, e.g.  $\delta_\theta = 0$ , or  $\sigma_{\theta\theta} = 0$ . The modeling involving dilational opening takes into account the effect of the tension coupling, and the result is a reduction in the critical loading for dislocation nucleation. A simple but approximate procedure to account for such a reduction is to use  $\gamma_{\text{us}}^{(r)}$ , i.e. the relaxed value instead of the unrelaxed value for  $\gamma_{\text{us}}$  in our formulation (Rice *et al.*, 1992). A full account of tension–shear coupling is presented in Sun *et al.* (1993).

The lattice potential  $\Phi(\delta_r, \delta_\theta = \text{constrained}, \delta_z)$  is a function of two independent variables, the slip displacements  $\delta_r$  and  $\delta_z$ , and is periodic along the  $\mathbf{s}(\phi)$  direction defined to be parallel to the Burgers vector and has a maximum called  $\gamma_{\text{us}}$ , the unstable stacking energy. The pathway for  $\boldsymbol{\delta}$  in the two dimensions of the slip displacements  $\delta_r$  and  $\delta_z$  going from zero, through the maximum point, and finally ending at one Burgers vector  $\mathbf{b}$  is a saddle-like path in the slip plane of the lattice potential  $\Phi(\delta_r, \delta_\theta = \text{constrained}, \delta_z)$  for full slip. In the direction which is perpendicular to the saddle path the lattice potential  $\Phi(\delta_r, \delta_\theta = \text{constrained}, \delta_z)$  rises rapidly. Assume that the slip displacement  $\boldsymbol{\delta}(r)$  is constrained strictly along  $\mathbf{s}(\phi)$ , in the so-called constrained path approximation (Rice, 1992),

$$\delta_x(r) = (\delta_s(r) \cos \phi, 0, \delta_s(r) \sin \phi) \equiv \delta_s(r) s_x(\phi), \quad (8)$$

where  $s_x(\phi) = (\cos \phi, 0, \sin \phi)$ . The assumption of the constrained path is excellent, especially in crystals for which the saddle path is straight, such as in Ni, Al and Ni<sub>3</sub>Al in the Shockley partial route.

The stress  $\sigma_{2z}(r)$  at a point  $r$  on the slip plane that is arbitrarily close to the crack tip is determined, by definition, by the stress intensity factor at the tip  $K_{x(\text{tip})}$  and may be singular, i.e.

$$\lim_{r \rightarrow 0} [\sqrt{2\pi r} \sigma_{2z}(r)] = K_{x(\text{tip})}. \quad (9)$$

The shear stress component  $\tau(r)$  along the  $\mathbf{s}(\phi)$  direction is  $\tau(r) = s_x(\phi) \sigma_{2z}(r)$ , which must be balanced by the lattice restoring force  $\tau(r) = s_x(\phi) \partial\Phi(\boldsymbol{\delta})/\partial\delta_x$ , where we recall that the  $\delta_x$  are set to  $s_x\delta_s$  in this expression. Since the lattice restoring force  $\tau(r)$  at the

tip cannot be arbitrarily large, the stress intensity factor along  $s(\phi)$  at the tip must vanish,

$$s_z(\phi)K_{z(\text{tip})} = K_{1(\text{tip})} \cos \phi + K_{3(\text{tip})} \sin \phi = 0. \quad (10)$$

Moreover, the stress intensity factor at the tip  $K_{z(\text{tip})}$  must be a linear superposition of applied  $K_x$  and the  $K_{z0}$  that are induced by the incipient dislocation zone slips  $\{\delta_\beta(r)\}$ . The slip zone  $\{\delta_\beta(r)\}$  is readily modeled as a continuous distribution of dislocations with Burgers vector  $b_\beta = -dr d\delta_\beta(r)/dr$ . The single line dislocation at  $r$  of Burgers vector  $b_\beta$  when the dislocation is coplanar with the crack plane produces a stress intensity factor  $K_{z0}$  (Rice, 1985),

$$K_{z0} = -\frac{1}{2\sqrt{2\pi r}} \Lambda_{z\beta}^{-1} b_\beta. \quad (11)$$

The stress intensity factor produced by the shear zone  $\{\delta_\beta(r)\}$  is then the integration over the entire continuous dislocation distribution. Consequently, we obtain

$$K_{z(\text{tip})} = K_x + \Lambda_{z\beta}^{-1} \hat{O} \delta_\beta(r), \quad (12)$$

where  $\hat{O}$  is an operator acting on  $\{\delta_\beta(r)\}$ ,

$$\hat{O} = \int_0^\infty -\frac{1}{2\sqrt{2\pi r}} \left[ -dr \frac{d}{dr} \right]. \quad (13)$$

We put in the constrained path approximation  $\delta_\beta(r) = s_\beta \delta_s(r)$  and obtain

$$K_{z(\text{tip})} = K_x + C \Lambda_{z\beta}^{-1} s_\beta(\phi), \quad (14)$$

where the term  $C$  arises from  $\hat{O}$  acting on  $\{\delta_\beta(r)\}$ ,

$$C = \int_0^\infty \frac{1}{2\sqrt{2\pi r}} \left[ dr \frac{d\delta_s(r)}{dr} \right]. \quad (15)$$

However, there exists another method to find the term  $C$  without having to solve for  $\delta_s(r)$ : combining (14) with (10) and solving for  $C$  gives

$$C = -\frac{s_z(\phi)K_x}{s_z(\phi) \Lambda_{z\beta}^{-1} s_\beta(\phi)}. \quad (16)$$

The stress intensity at the tip is completely determined by (14) and (16), and is combined with (7). After a few algebraic steps, we arrive at

$$g \equiv \frac{[s_z(\phi)K_x]^2}{s_z(\phi) \Lambda_{z\beta}^{-1} s_\beta(\phi)} = \Phi(\delta_{\text{tip}}), \quad (17)$$

where we have used the fact that the matrices  $\Lambda_{z\beta}$  and  $\Lambda_{z\beta}^{-1}$  are symmetric.

The variable  $g$  in (17) would become  $G$ , the crack extension force, under special circumstances provided that the matrix  $\Lambda_{z\beta}$  is diagonal and: (1) either for pure edge dislocation nucleation under pure  $K_I = K_{II}$  loading, or (2) pure screw dislocation nucleation under pure  $K_3 = K_{III}$  loading. The condition for dislocation nucleation in these two special cases is then  $G = \gamma_{\text{us}}$ , which is the same as in the isotropic formulation.

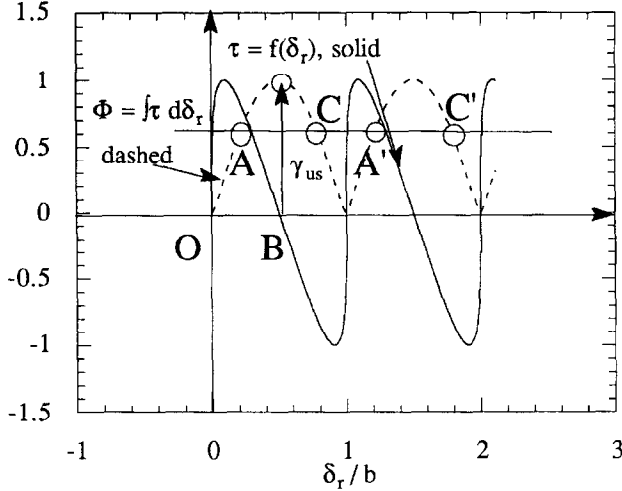


Fig. 3. The periodic relation of shear stress (solid curve) and its associated potential (dashed curve) versus the slip displacement within the Peierls concept. Each is scaled by its maximum and the displacement by  $b$ .

The relation expressed by (17) connects the solution of the shear zone  $\{\delta_\beta(r)\}$  to the applied loading  $\{K_x\}$ . Due to the periodic nature of the lattice potential  $\Phi(\delta)$  in the constrained path expressed by  $\delta_x(r) = s_x(\phi) \delta_s(r)$  in the slip process, there correspond multiple solutions  $A, C, A', C', \dots$ , to one set of loadings  $K_x$ , as shown in Fig. 3. Point  $A$  represents the stable solution, while point  $C$  is the unstable after-critical solution for the incipient shear zone of the first dislocation. The critical solution corresponds to point  $B$ , when the lattice potential  $\Phi(\delta)$  takes the maximum value  $\gamma_{us}$ . The solutions  $A'$  and  $C'$ , etc., correspond to the second dislocation nucleation processes, respectively. The dislocation nucleation criterion for the first dislocation is

$$s_x(\phi) K_x = \sqrt{\gamma_{us} p(\phi)}, \tag{18}$$

where we have defined  $p(\phi) \equiv s_x(\phi) \Lambda_{x\beta}^{-1} s_\beta(\phi)$ . It is interesting to note that the term  $s_x(\phi) K_x$  of combination of shear  $K_1$  and anti-plane shear loadings  $K_3$  can be regarded as the shear stress intensity factor along the  $s_x(\phi)$  direction in the slip plane.

We note that (14) can be rewritten as

$$\Lambda_{\beta x} K_{x(\text{tip})} - \Lambda_{\beta x} K_x = C s_\beta(\phi). \tag{19}$$

The term  $\Lambda_{\beta x} K_x$  determines the displacement discontinuity between the crack surfaces behind the crack tip,

$$\Delta u_\beta(r) = u_\beta^+(r) - u_\beta^-(r) = 4\sqrt{2r/\pi} \Lambda_{\beta x} K_x, \tag{20}$$

in the absence of any shear zone  $\{\delta_\beta(r)\}$  (Rice, 1985). Thus,  $\Lambda_{\beta x} K_x$  can be termed the displacement intensity factors in analogy with the stress intensity factor  $K_x$ . Equation (19) can also be interpreted as follows: the displacement intensity factors  $\Lambda_{\beta x} K_x$  remain unchanged near the tip, along both the crack opening direction and the

direction perpendicular to the  $s_x(\phi)$ , for partial relief of singular stress in the constrained path approximation.

### *Nucleation of dissociated dislocations on coincidental crack and slip planes*

Frequently, dissociated partial dislocations are formed in metals, e.g. Shockley partials in fcc crystals, and partials connected by faulted planes such as the anti-phase boundary (APB), complex stacking fault (CSF) and superlattice intrinsic stacking fault (SISF) in intermetallics. It is likely that dislocation emission in fcc materials consists of sequentially emitted partials rather than the full dislocation.

We consider now the emission of paired partials in the same manner as Rice (1992), but using anisotropic elasticity, understanding that the interpretation of those formulae are to be corrected as in a note appended to Rice *et al.* (1992) to account for the partials forming in a definite ordered sequence rather than competitively. The slip plane is presumed to be coplanar with the crack surfaces for simpler mathematical manipulations. The first partial is labeled  $A$ , with slip direction at angle  $\phi_A$  with the  $r$  direction in the slip plane, while the second partial is labeled  $B$ , with slip direction at angle  $\phi_B$ .

The emission of the first partial occurs in an anisotropic medium when the nucleation condition expressed in (18) is reached,

$$K_A \equiv s_x(\phi_A)K_x = \sqrt{\gamma_{us}p(\phi_A)} \equiv K_{AC}. \quad (21)$$

The emitted partial has two effects on the nucleation of the second: (1) shielding of the loading and (2) offset of the lattice potential from zero to the value of the stacking fault energy so that the energy barrier for the second partial nucleation is  $(\gamma_{us} - \gamma_{sf})$ .

The shielding of the loading depends on the location of the emitted partial as expressed by (11). The emitted partial dislocation will be treated as a line defect; the self-consistency is ensured by the fact that it is far away from the shear zone of the second partial at the crack tip. Its stable equilibrium position is found from the condition that the force exerted on it in the slip plane vanishes (the larger of the two roots of the following equation), i.e. the balance of the Peach–Köhler force and the attractive forces of the stacking fault energy and the image force in the slip plane,

$$f_A = K_A b_A / \sqrt{2\pi r_A} - \gamma_{sf} + f_r = 0, \quad (22)$$

where  $f_r$  is the image force on the partial dislocation in a slip plane and has been derived by Asaro (1975) and Rice (1985),

$$f_r = -\frac{b_A^2 s_x(\phi_A) \Lambda_{xy}^{-1} s_x(\phi_A)}{8\pi r_A} = -\frac{b_A^2 p(\phi_A)}{8\pi r_A}. \quad (23)$$

The glide motion of the first partial also experiences a friction force  $\sigma_p b_A$  from lattice resistance, the Peierls stress  $\sigma_p$ ; hence the term  $\gamma_{sf}$  should be replaced by  $(\gamma_{sf} + \sigma_p b_A)$  in (22). The Peierls stress  $\sigma_p$  is of order  $10^{-4}$  to  $10^{-2} \mu_{\text{slip}}$  (Hirth and Lothe, 1982). For fcc metals, we estimate  $\sigma_p b_A$  to be  $10^{-4} \mu_{\text{slip}} b_A$  and  $\gamma_{sf}$  to be  $1/3 \gamma_{us} \approx 0.01 \mu_{\text{slip}} b_A$  (Rice, 1992; Rice *et al.*, 1992) so that the lattice friction  $\sigma_p b_A$  is about 1% of  $\gamma_{sf}$ , which is

justifiably neglected for fcc metals here. For the position of the first partial, a relation is found by solving (22) in connection with (21) and (23),

$$\frac{b_A}{2\sqrt{2\pi r_A}} = \frac{K_A \left[ 1 - \sqrt{1 - \left(\frac{K_{AC}}{K_A}\right)^2 \left(\frac{\gamma_{sf}}{\gamma_{us}}\right)} \right]}{p(\phi_A)}. \quad (24)$$

Its position is estimated to be 10–50 times  $b_A$  away from the tip. The stress intensity factor is now shielded by the emitted first partial dislocation according to (11),

$$K_x^* = K_x - \left( \frac{b_A}{2\sqrt{2\pi r_A}} \right) \Lambda_{z\beta}^{-1} s_\beta(\phi_A). \quad (25)$$

The shear stress intensity factor along the  $s_z(\phi_B)$  direction is  $K_B \equiv s_z(\phi_B) K_x$  and for the screened stress intensity factor  $K_B^* \equiv s_z(\phi_B) K_x^*$ ,

$$K_B^* = K_B - \eta(\phi_B, \phi_A) K_A + \eta(\phi_B, \phi_A) \sqrt{K_A^2 - \gamma_{sf} p(\phi_A)}, \quad (26)$$

where

$$\eta(\phi_B, \phi_A) = \frac{s_z(\phi_B) \Lambda_{z\beta}^{-1} s_\beta(\phi_A)}{s_z(\phi_A) \Lambda_{z\beta}^{-1} s_\beta(\phi_A)} = \frac{s_z(\phi_B) \Lambda_{z\beta}^{-1} s_\beta(\phi_A)}{p(\phi_A)}. \quad (27)$$

The emission of the second partial dislocation occurs when

$$K_B^* = \sqrt{(\gamma_{us} - \gamma_{sf}) p(\phi_B)}. \quad (28)$$

The two effects of the emitted first partial have been incorporated into the nucleation condition expressed in (28).

#### *Approximate nucleation condition in the case of a tilted slip plane*

If the slip plane is inclined at an angle  $\theta$  with the crack plane, the exact solution can only be obtained by numerical methods [see Beltz (1992), Rice *et al.* (1992) and Sun *et al.* (1993) and also the next section]. We would project the singular stress concentration and the  $\Lambda_{z\beta}$  matrix from the main crack onto the slip plane, then treat such a projected case as if the crack were coplanar with and just behind the slip plane. This method of projection is only rudimentary, and must be checked by the numerical solution. We will observe that this projection method is justified, though approximate.

The approximation occurs in two steps. First, we adopt the concept of the *effective stress intensity factors*  $K_x^{\text{eff}}$  as proposed by Rice (1992). These effective stress intensity factors  $K_x^{\text{eff}}$  are defined through the stress components  $\sigma_{\theta z}(r)$  in the slip plane with  $\alpha = (r, \theta, z)$  from the general loading  $\mathbf{K} = (K_1, K_2, K_3) = (K_{II}, K_I, K_{III})$  on the main crack,

$$\sigma_{\theta z}(r) = \frac{F_{z\beta}(\theta) K_\beta}{\sqrt{2\pi r}}, \quad (29)$$

such that

$$\sigma_{\theta z}(r) \equiv \frac{K_x^{\text{eff}}}{\sqrt{2\pi r}}. \tag{30}$$

We have

$$K_x^{\text{eff}} = F_{z\beta}(\theta) K_\beta. \tag{31}$$

Secondly, we find the proper  $\Lambda_{z\beta}^{(0)}$  matrix for crack extension force  $G_r$  for a crack extending along the  $r$  direction such that  $G_r = K_x^{\text{eff}} \Lambda_{z\beta}^{(0)} K_\beta^{\text{eff}}$ . The  $\Lambda_{z\beta}^{(0)}$  matrix is related to the  $\Lambda_{z\beta}$  matrix by

$$\Lambda_{z\beta}^{(0)} = R_{z\beta} \Lambda_{\delta\gamma} R_{\beta\gamma}, \tag{32}$$

where  $\mathbf{R}$  is the rotation matrix,

$$\mathbf{R} = \begin{bmatrix} \cos \theta & \sin \theta & 0 \\ -\sin \theta & \cos \theta & 0 \\ 0 & 0 & 1 \end{bmatrix}. \tag{33}$$

It is easily shown that the inverse of the  $\Lambda_{z\beta}^{(0)}$  matrix,  $\Lambda_{z\beta}^{(0)-1} = R_{z\beta} \Lambda_{\delta\gamma}^{-1} R_{\beta\gamma}$ .

The dislocation nucleates on the inclined plane when the condition expressed by (18) is satisfied, but here in the context of the effective stress intensity concept and the  $\Lambda_{z\beta}^{(0)}$  matrix for the inclined plane, that is

$$s_x(\phi) K_x^{\text{eff}} = \sqrt{\gamma_{\text{us}} p(\phi, \theta)}, \tag{34}$$

where  $p(\phi, \theta) = s_x(\phi) \Lambda_{z\beta}^{(0)-1} s_\beta(\phi)$ .

### INTEGRAL EQUATION FORMULATION FOR THE PROBLEM OF DISLOCATION EMISSION FROM A CRACK TIP

In the previous section, the dislocation emission criterion was approximately obtained by the effective stress intensity factor  $K_x^{\text{eff}}$  and  $\Lambda_{z\beta}^{(0)}$ , obtained by the projection method, when the slip plane is inclined with respect to crack planes. Should the normal stress also be taken into account, the critical nucleation criterion can no longer be determined by the  $J$ -integral even in the coplanar slip and crack planes case, but only be determined exactly by numerical methods. We now present exact treatments for the general cases involving inclined slip planes and mixed edge and screw components, including tension–shear coupling.

#### *The combined tension–shear model*

Suppose an incipient profile  $\{\delta_r(r), \delta_\theta(r), \delta_z(r)\}$  develops on an inclined slip plane, in response to the stress concentration at the crack tip under combined  $K_x$  loading, which is similar to Fig. 1. We assume that the profile is predominantly shear, with small opening displacements.

The incipient profile  $\{\delta_x(s)\}$  is, as before, modeled here as a continuous distribution of an individual dislocation at location  $s$  of an infinitesimal Burgers vector

$[-(d\delta_\alpha(s)/ds)ds]$ , which in turn will exert stresses  $\sigma_{\theta\alpha}(r) = g_{\alpha\beta}(r, s; \theta)$   $[-(d\delta_\beta(s)/ds)ds]$  on a point  $r$  along the slip plane. Therefore, the Green's functions  $g_{\alpha\beta}(r, s; \theta)$  so defined can be obtained by solutions of a line dislocation interacting with the crack tip in the anisotropic linear elastic medium. Some details are presented in the Appendix. The force balance at a point  $r$  along the slip plane gives equations of equilibrium,

$$\sigma_{\theta\alpha}[\delta(r)] = \sigma_{\theta\alpha}^0(r) + \int_0^\infty g_{\alpha\beta}(r, s, \theta) \left[ -\frac{d\delta_\beta(s)}{ds} ds \right], \tag{35}$$

where  $(\alpha, \beta) = (r, \theta, z)$ , but also denoted as (1, 2, 3), and  $\sigma_{\theta\alpha}^0(r)$ , the unrelaxed stress from the crack loading  $K_\alpha$ , are given as  $\sigma_{\theta\alpha}^0(r) = F_{\alpha\beta}(\theta)K_\beta/\sqrt{2\pi r}$ , as in the previous section.

The term  $\sigma_{\theta\alpha}[\delta(r)]$  is the lattice restoring shear and tension stress against the displacement discontinuities across the slip plane at point  $r$ , with which a potential  $\Phi[\delta_\alpha(r)]$  is associated, such that

$$\sigma_{\theta\alpha}[\delta(r)] = \frac{\partial\Phi[\delta(r)]}{\partial\delta_\alpha(r)}. \tag{36}$$

Equations (35) and (36) constitute a complete set of equations to be solved simultaneously.

We remark about properties of the Green's functions  $g_{\alpha\beta}(r, s; \theta)$ . It can be shown that

$$g_{\alpha\beta}(r, s; \theta) = \frac{1}{4\pi} \sqrt{\frac{s}{r}} \frac{[\Lambda_{\alpha\beta}^{(\theta)-1} + h_{\alpha\beta}(r/s, \theta)]}{r-s}, \tag{37}$$

where the following properties of the function  $h_{\alpha\beta}(t, \theta)$  are of interest: first,

$$h_{\alpha\beta}(1, \theta) = 0, \tag{38}$$

in order to have proper stress fields in the linear elastic medium near the dislocation point  $s$ . Furthermore, the Rice–Thomson image force theorem for a dislocation line at a crack tip implies that  $\partial h_{\alpha\beta}(t = 1, \theta)/\partial t$  is antisymmetric for indices  $\alpha$  and  $\beta$ , i.e.

$$\partial h_{rr}(t = 1, \theta)/\partial t = 0, \tag{39a}$$

$$\partial h_{\theta\theta}(t = 1, \theta)/\partial t = 0, \tag{39b}$$

$$\partial h_{zz}(t = 1, \theta)/\partial t = 0, \tag{39c}$$

$$\partial h_{r\theta}(t = 1, \theta)/\partial t + \partial h_{\theta r}(t = 1, \theta)/\partial t = 0, \tag{39d}$$

$$\partial h_{rz}(t = 1, \theta)/\partial t + \partial h_{zr}(t = 1, \theta)/\partial t = 0, \tag{39e}$$

$$\partial h_{\theta z}(t = 1, \theta)/\partial t + \partial h_{z\theta}(t = 1, \theta)/\partial t = 0. \tag{39f}$$

The conditions given by (38) and (39) are trivially satisfied for  $\theta = 0$ , i.e.  $h_{\alpha\beta}(r/s, 0) = 0$ . Further details regarding the stress functions  $g_{\alpha\beta}(r, s; \theta)$  are presented in the Appendix.

We also apply the constrained slip path approximation here. Let the slip be constrained to be along the direction  $\mathbf{s}$  (the same as  $\mathbf{b}$ ) that makes an angle  $\phi$  with the  $\mathbf{r}$

axis in the slip plane,  $\delta_x(r) = [\delta_s(r) \cos \phi, \delta_\theta(r), \delta_s(r) \sin \phi]$  and the stress  $\tau = \sigma_{\theta r} \cos \phi + \sigma_{\theta z} \sin \phi$  and  $\sigma = \sigma_{\theta\theta}$ . We seek the condition under which the profile becomes unstable, after which a dislocation emerges and moves away from the crack tip until being stopped by the lattice resistance, the Peierls stress  $\sigma_p$ , or by interactions with distant dislocations, etc. We obtain the following equations:

$$\tau[\delta_s(r), \delta_\theta(r)] = \frac{K_\tau^{\text{eff}}}{\sqrt{2\pi r}} - \int_0^z \bar{g}_{11}(r, s; \theta, \phi) \frac{d\delta_s(s)}{ds} ds - \int_0^z \bar{g}_{12}(r, s; \theta, \phi) \frac{d\delta_\theta(s)}{ds} ds, \quad (40)$$

$$\sigma[\delta_s(r), \delta_\theta(r)] = \frac{K_\sigma^{\text{eff}}}{\sqrt{2\pi r}} - \int_0^z \bar{g}_{21}(r, s; \theta, \phi) \frac{d\delta_s(s)}{ds} ds - \int_0^z \bar{g}_{22}(r, s; \theta, \phi) \frac{d\delta_\theta(s)}{ds} ds, \quad (41)$$

where  $K_\tau^{\text{eff}} = \sqrt{2\pi r} [\cos \phi \sigma_{\theta r}^0(r, \theta) + \sin \phi \sigma_{\theta z}^0(r, \theta)] = s_x(\phi) F_{z\beta}(\theta) K_\beta$  and  $K_\sigma^{\text{eff}} = \sqrt{2\pi r} \sigma_{\theta\theta}^0(r, \theta) = F_{2\beta}(\theta) K_\beta$ . These are defined for the singular stresses  $\sigma_{\theta r}^0$ ,  $\sigma_{\theta z}^0$  and  $\sigma_{\theta\theta}^0$  at the crack tip under external loading before the emergence of the incipient profile. The functions  $\bar{g}_{11}$ ,  $\bar{g}_{12}$ ,  $\bar{g}_{21}$  and  $\bar{g}_{22}$  are stress functions for a straight dislocation at a crack tip:  $\bar{g}_{11}(r, s; \theta) = s_x(\phi) g_{z\beta}(r, s; \theta) s_\beta(\phi)$ ,  $\bar{g}_{12}(r, s; \theta) = s_z(\phi) g_{z2}(r, s; \theta)$ ,  $\bar{g}_{21}(r, s; \theta) = g_{2z}(r, s; \theta) s_x(\phi)$  and  $\bar{g}_{22}(r, s; \theta) = g_{22}(r, s; \theta)$ . All of these terms and functions can be obtained from the singular field of a loaded crack tip and solution of a dislocation near a crack tip using the anisotropic elasticity formulation see e.g., Atkinson (1966), Asaro (1975) and Suo (1989).

The terms  $\tau[\delta_s(r), \delta_\theta(r)]$  and  $\sigma[\delta_s(r), \delta_\theta(r)]$  are lattice restoring shear and tension stresses against the displacement discontinuities across the slip plane: a potential  $\Phi[\delta_s(r), \delta_\theta(r)]$  is assumed to exist, such that

$$\tau[\delta_s(r), \delta_\theta(r)] = \frac{\partial \Phi[\delta_s(r), \delta_\theta(r)]}{\partial \delta_s(r)}, \quad (42)$$

$$\sigma[\delta_s(r), \delta_\theta(r)] = \frac{\partial \Phi[\delta_s(r), \delta_\theta(r)]}{\partial \delta_\theta(r)}. \quad (43)$$

Modeling of the constitutive law  $\Phi[\delta_s(r), \delta_\theta(r)]$  from EAM results for Ni, Al, Ni<sub>3</sub>Al, and Fe, from sources noted above, and from density functional studies of Si by Kaxiras and Duesbery (1993), Duesbery *et al.* (1990), Huang *et al.* (1991) and Huang (1992) have been provided in Sun *et al.* (1993), Rice *et al.* (1992) and Sun (1993). The same potential from such atomic models is used here. The analytic representations of the stresses and the potentials can be found in Beltz and Rice (1991), Rice *et al.* (1992) and Sun *et al.* (1993). Equations (40)–(43) constitute a complete set of equations which can be solved jointly to determine the critical loading and corresponding incipient configuration. The solutions are obtainable numerically, by use of the Newton–Raphson method and Chebyshev polynomials of the second kind [see, e.g., Erdogan (1975) and Erdogan and Gupta (1972)].

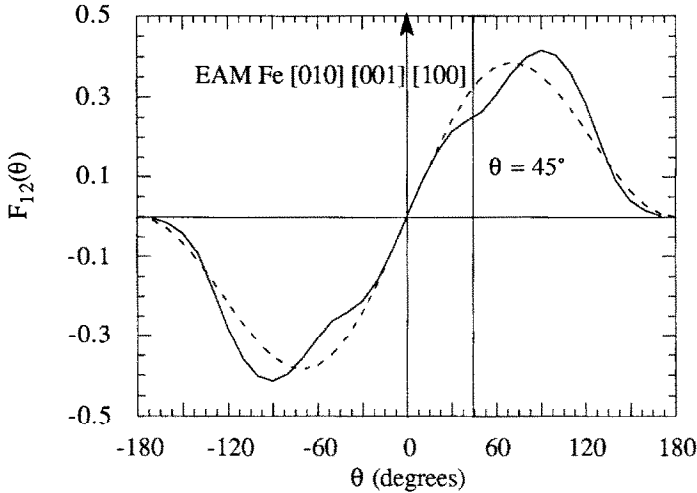


Fig. 4. The angular distribution of the singular shear stress  $\sigma_{\theta r}(r, \theta)\sqrt{2\pi r}/K_I = F_{12}(\theta)$  near crack tip  $A$  under mode I loading in EAM-Fe; anisotropic versus isotropic formulations.

*The shear-only model*

In the shear-only model, where only the slip displacements and shear stresses are considered, there exists a simpler set of equations,

$$\tau[\delta_s(r)] = \frac{K_{\tau}^{eff}}{\sqrt{2\pi r}} - \int_0^{\infty} \bar{g}_{11}(r, s; \theta, \phi) \frac{d\delta_s(s)}{ds} ds. \tag{44}$$

Equation (44) is accompanied by a sinusoidal law

$$\tau(\Delta_s) = (\pi\gamma_{us}/b) \sin(2\pi\Delta_s/b), \tag{45}$$

where  $\Delta_s$  is the relative atomic sliding displacement between the two adjacent slipping atomic layers, which is related to  $\delta_s$ , the displacement discontinuity across the slip plane, by

$$\delta_s = \Delta_s - (b/2\pi) \sin(2\pi\Delta_s/b). \tag{46}$$

EXACT RESULTS AND CONCLUSIONS

*The significance of anisotropic elasticity*

The anisotropic effect is surveyed initially in three parts. It appears in the angular dependence of the singular shear stress  $\sigma_{\theta r}^0(r, \theta)$  near a crack tip under pure tensile loading, i.e.  $F_{12}(\theta)$  in previous notation. In isotropic elasticity,  $F_{12}(\theta) = \cos^2(\theta/2) \sin(\theta/2)$ , corresponding to the dashed curves in Figs 4–7. Figures 4 and 5 show the comparison of anisotropy with isotropy for a crack growing in the [010] direction, with crack front along [100] and crack planes on (001) planes (crack  $A$ ) in EAM-Fe

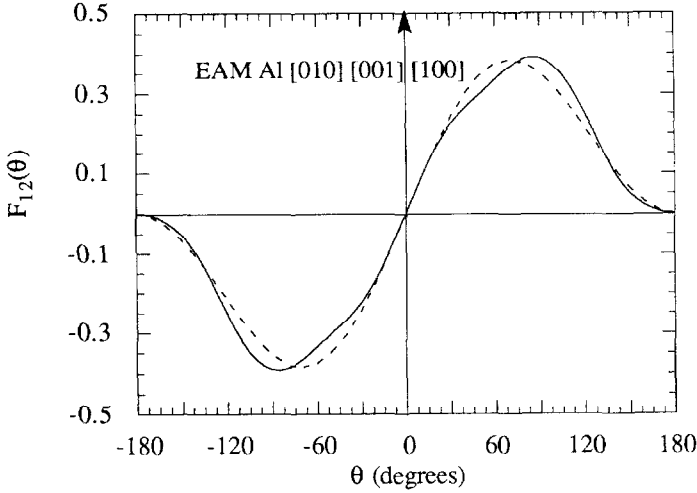


Fig. 5. The angular distribution of the singular shear stress  $\sigma_{\theta}(r, \theta) \sqrt{2\pi r}/K_I = F_{12}(\theta)$  near crack tip *A* under mode I loading in EAM-Al: anisotropic versus isotropic formulations.

and EAM-Al. We note that the anisotropic results have significantly different shapes from the isotropic ones, more so in bcc than fcc. Also, Figs 6 and 7 show results for EAM-Fe using crack orientations *B* ( $[\bar{1}10]$ - $[001]$ - $[111]$ ) and *C* ( $[011]$ - $[0\bar{1}1]$ - $[100]$ ).

Figure 8 shows the function  $\bar{g}_{11}(r, s, \theta) b$ , which is part of the equation for  $\sigma_{\theta}(r)$  and is the key function in the shear-only model, for crack *A*. Here, the slip plane is tilted so that  $\theta = 45^\circ$ , as is appropriate for Fe. The figure shows the Cauchy singularity ( $1/x$ ) as implied by (36). It is seen that a similar shape of the function results

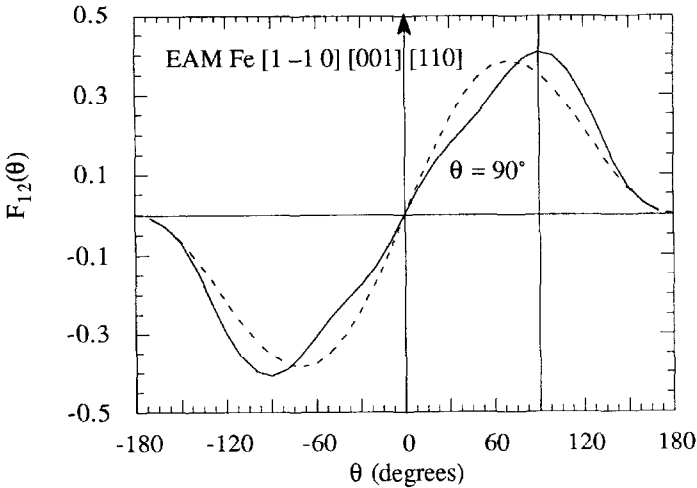


Fig. 6. The angular distribution of the singular shear stress  $\sigma_{\theta}(r, \theta) \sqrt{2\pi r}/K_I = F_{12}(\theta)$  near crack tip *B* under mode I loading in EAM-Fe: anisotropic versus isotropic formulations.

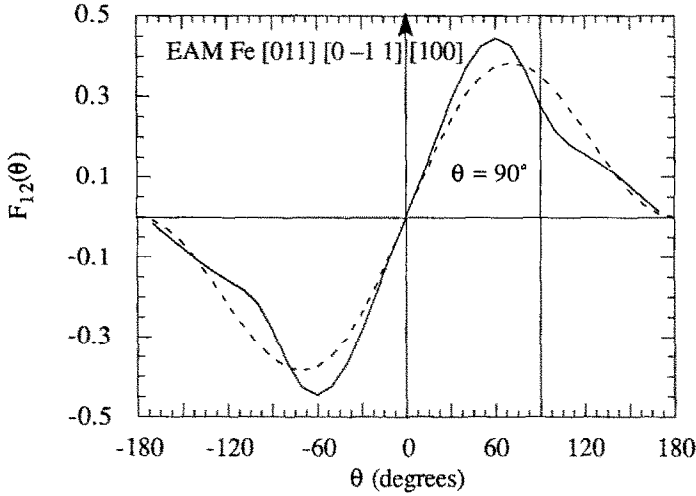


Fig. 7. The angular distribution of the singular shear stress  $\sigma_{\theta r}(r, \theta) \sqrt{2\pi r}/K_I = F_{12}(\theta)$  near crack tip  $C$  under mode I loading in EAM-Fe; anisotropic versus isotropic formulations.

for anisotropic and isotropic formulations, though their numerical values are not identical.

Finally, the critical loading  $G_d$  as determined in the shear-only model is shown in Fig. 9 as a function of inclination angle  $\theta$  of the slip plane, in anisotropic and isotropic formulations for crack  $A$  in EAM-Fe under pure mode I loading and for emission of a dislocation of pure edge character. The anisotropic effect is numerically significant; it differs from the curve obtained using isotropic elasticity, which can overestimate or underestimate the anisotropic results, depending on  $\theta$ .

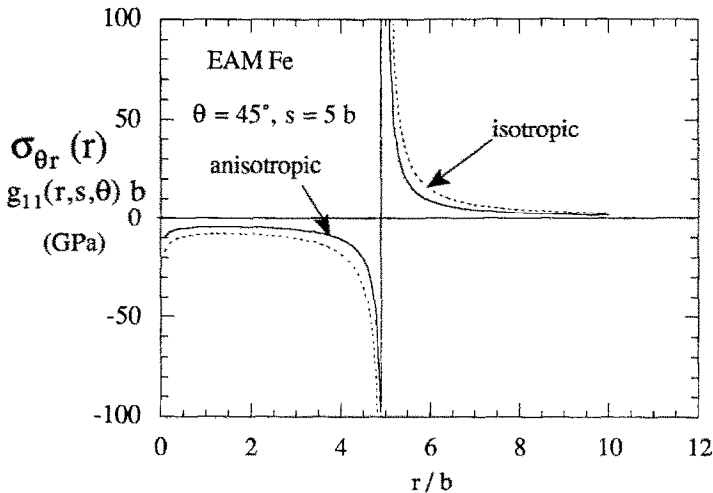


Fig. 8. The distribution of the stress  $\sigma_{\theta r}(r, \theta) = g_{11}(r, s, \theta) b$  produced by an edge dislocation of Burgers vector  $b$  located at  $s = 5b$  on a  $45^\circ$  tilted slip plane in crack tip  $A$ ; anisotropic versus isotropic formulations.

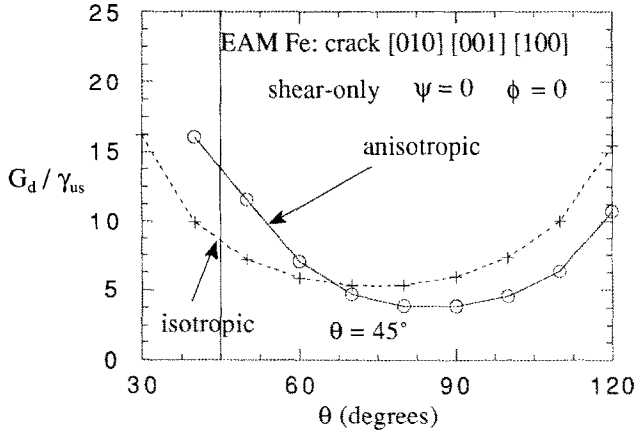


Fig. 9. The critical load  $G_d$  as a function of inclination angle  $\theta$  for dislocation emission from crack  $A$  in EAM-Fe under mode I loading as determined in the shear-only model; anisotropic versus isotropic formulations.

*A survey of anisotropic effects on critical loadings*

Consider the case where the slip plane is coplanar with the crack plane and  $\phi = 0$ . As mentioned previously, the critical loading  $G_d$  for dislocation emission is equal to  $\gamma_{us}$  in the shear-only model. The tension effect on dislocation emission in model  $A$ , using anisotropic elasticity with EAM-Fe, is analysed by varying the amount of tensile loading with respect to shear loading,  $\psi = \arctan (K_{II}/K_I)$ . Figure 10 shows the results. The critical  $G_d(\psi)$  in the isotropic formulation, taken from Fig. 3.2(b) of Sun *et al.* (1993), accompanies those in the anisotropic formulation. It shows that by the proper

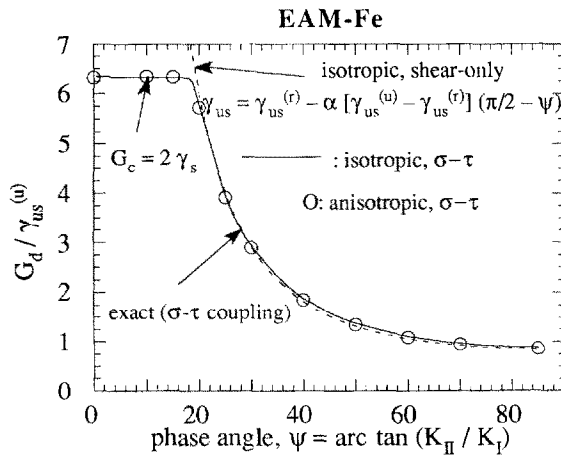


Fig. 10. The critical load  $G_d$  as a function of the phase angle  $\psi$  of loading for edge dislocation emission from crack  $A$  in EAM-Fe on a coplanar slip plane, as determined in the tension–shear coupled model: anisotropic versus isotropic formulations. Fitting by the isotropic shear-only model with the tension reduced unstable stacking energy  $\gamma_{us}(\psi)$  is also shown.

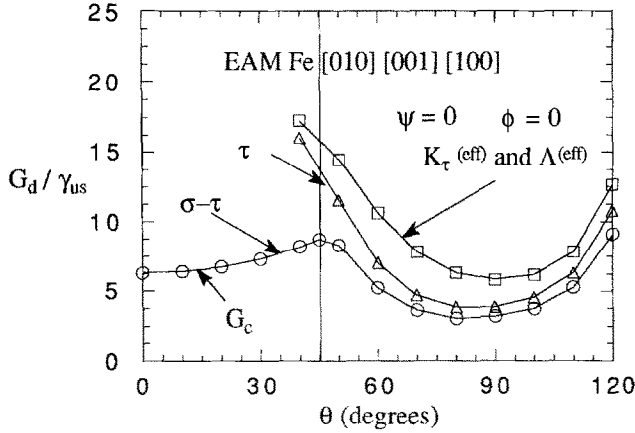


Fig. 11. The critical loading  $G_d$  as a function of the inclination angle  $\theta$  for edge dislocation emission from crack  $A$  in EAM-Fe under mode I loading, as determined in the effective approximation; shear-only and tension–shear coupled models (scaled by  $\gamma_{us}^{(u)}$ ), anisotropic formulation.

treatment of anisotropic effects, the two formulations render almost the same results in the tension–shear coupling model. That seems more general than the following case: as was shown previously, in the case of orthotropic crack and coplanar crack and slip planes, both formulations would predict the same  $G$  value for edge dislocation emission in the shear-only model. As in Sun *et al.* (1993) with isotropic elasticity, the combined tension–shear model in the anisotropic formulation is fitted by the modified shear-only model, which uses the tension reduced  $\gamma_{us}(\psi)$ , namely,

$$G_d(\psi) = \gamma_{us}(\psi) / \sin^2 \psi, \tag{47}$$

where  $\gamma_{us}(\psi) = \gamma_{us}^{(r)} - \alpha[\gamma_{us}^{(u)} - \gamma_{us}^{(r)}](\pi/2 - \psi)$  for tension reduction. The modified shear-only model gives a good description. The same  $\alpha$  coefficient applies to both anisotropic and isotropic results. For EAM-Fe,  $\alpha$  is 0.841.

We further illustrate anisotropic effects for the case of a tilted slip plane making an inclination angle  $\theta$  with the crack plane when the crack is loaded in pure mode I. Results are presented for crack orientations  $A$ ,  $B$  and  $C$  in bcc EAM-Fe. Here the angle  $\theta$  ranges from  $40^\circ$  to  $120^\circ$  and angle  $\phi = 0^\circ$ . These  $\theta$  and  $\phi$  angles may not be the actual inclination and screw/edge mixing angles for a slip system in the crack orientation models  $A$ ,  $B$  and  $C$ ; we merely intend to show the dependence of the critical loading  $G_d$  upon anisotropic medium effects. The critical loading as a function of inclination angle  $\theta$ , expressed as  $G_d$  as determined in the combined tension–shear model (labeled  $\sigma - \tau$ ), shear-only model (labeled  $\tau$ ) and effective shear intensity factor model in the anisotropic elasticity formulation for model  $A$  is shown in Fig. 11, crack  $B$  in Fig. 12 and  $C$  in Fig. 13. The effective stress approximation gives a good description of the general shape, although it overestimates the loading by about 20%, compared to the numerical results of the shear-only model. The combined tension and shear model further reduces the loading by 10–15%.

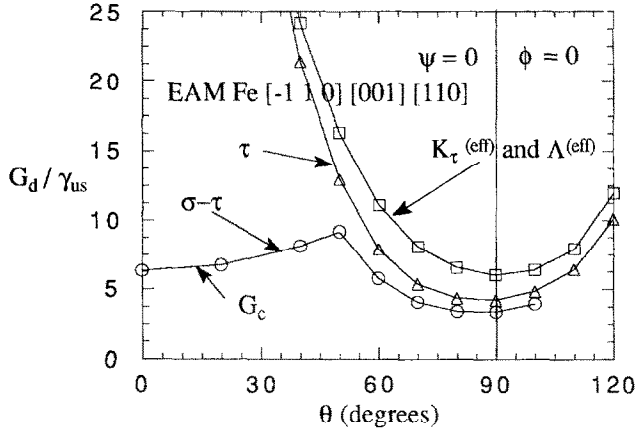


Fig. 12. The critical loading  $G_d$  as a function of the inclination angle  $\theta$  for edge dislocation emission from crack  $B$  in EAM-Fe under mode I loading, as determined in the effective approximation; shear-only and tension–shear coupled models (scaled by  $\gamma_{us}^{(0)}$ ), anisotropic formulation.

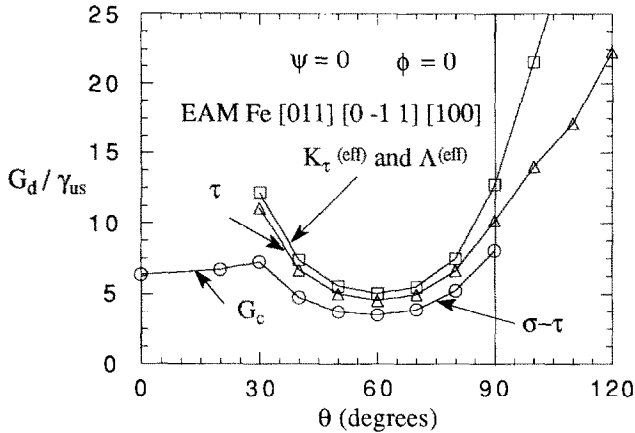


Fig. 13. The critical loading  $G_d$  as a function of the inclination angle  $\theta$  for edge dislocation emission from crack  $C$  in EAM-Fe under mode I loading, as determined in the effective approximation; shear-only and tension–shear coupled models (scaled by  $\gamma_{us}^{(0)}$ ), anisotropic formulation.

#### A scheme for rough estimates

From the above discussions, we devise a procedure for calibrating the effective stress intensity factor method on the basis of exact numerical solutions, including tension–shear coupling. Let the critical stress intensity factor  $K_d$ , as estimated from the effective method, be multiplied by a factor  $\eta$  so as to equal the shear-only  $K_d$ . The  $\eta$  factor ranges from 0.86 to 0.95. The tension–shear coupling is handled by the tension reduced  $\gamma_{us}(\psi)$  value, which was treated in Sun *et al.* (1993), though in isotropic formulations. It was shown that this tension-reduced unstable stacking energy is valid for EAM-Ni, -Al, -Fe and -Ni<sub>3</sub>Al, but less well for DFT/LDA-Si. We expect that it will work equally well in the anisotropic formulation.

Table 2. Critical loading  $G_d/\gamma_{us}^{(r)}$  for dislocation emission from an anisotropic crack under mode I loading

Material	Crack orient	$(\theta, \phi)$ ( $^\circ$ )	Eff.	$\tau$	$\sigma-\tau$	$\eta$ recipe
Fe	A	(-45, 35.3)	29.96	27.40	10.58‡	0.9577
Fe	B	(-90, 54.7)	11.85	9.144	8.106	0.8785
Fe	C	(-90, 35.3)	23.80	19.48	17.75	0.9058
Ni	D	(54.7, 60)	32.02	29.06	22.09	0.9528
Ni	E	(35.3, 0)	10.48	9.92	8.103	0.9720
Al	D	(54.7, 60)	28.40	25.72	19.85	0.9518
Al	E	(35.3, 0)	11.54	10.89	8.705	0.9716
Al	F†	(90, 30)	10.71	8.315	7.664	0.8813
Ni <sub>3</sub> Al	D	(54.7, 60)	30.27	28.43	17.91‡	0.9557
Ni <sub>3</sub> Al	E	(35.3, 0)	11.05	10.40	8.342	0.9698
Si, glide	D	(54.7, 60)	29.13	26.70	2.959‡	0.9574
Si, glide	E	(35.3, 0)	11.66	10.89	2.041‡	0.9665
Si, glide	F†	(90, 30)	10.27	7.879	5.784	0.8758
Si, glide	G†	(70.5, 0)	6.521	5.253	3.226	0.8975
Si, glide	G†	(70.5, 60)	20.56	17.97	4.729‡	0.9348
Si, shuffle	D	(54.7, 30)	11.26	9.560	2.642‡	0.9213
Si, shuffle	E	(35.3, 30)	14.54	13.69	1.979‡	0.9702
Si, shuffle	F†	(90, 0)	8.243	6.166	6.345	0.8649
Si, shuffle	G†	(70.5, 30)	8.082	6.669	3.882‡	0.9084

† The in-plane elasticity is taken to be decoupled from the anti-plane elasticity to simplify the treatment, which is only approximate.

‡ The instability may correspond to decohesion along the inclined slip plane rather than dislocation emission.

We can summarize individually for each common crack orientation and the easiest slip system (i.e.  $\theta, \phi$  angles) listed in Table 1. The critical loading for dislocation emission under mode I loading is summarized in Table 2, as determined by the three methods. The critical condition under pure mode I loading was determined via the numerical procedure, the shear-only model and the effective model. By comparing two solutions for the same situation, we obtain the  $\eta$  coefficient for each crack orientation and slip system (i.e. angles  $\theta$  and  $\phi$ ). Here we assume the coefficient  $\eta$  is unique for each set of  $\theta$  and  $\phi$  angles, which approximately holds true for every material. The tension–shear coupling would reduce the loading at the critical condition, and the results are also presented in Table 2. The tension–shear coupling is approximated by the tension reduced  $\gamma_{us}$ . The tension reduced  $\gamma_{us}$  in terms of the phase angle  $\psi$  is

$$\gamma_{us}(\psi) = \gamma_{us}^{(r)} - \alpha[\gamma_{us}^{(u)} - \gamma_{us}^{(r)}](\pi/2 - \psi), \quad (48)$$

where the phase angle is for the effective shear versus tensile stress intensity, i.e.

$$\psi = \arctan(K_t/K_\sigma). \quad (49)$$

The coefficient  $\alpha$  is from Sun *et al.* (1993) for tension–shear coupling. It is different for each EAM material and slip system. In particular,  $\alpha$  has the values 1.323, 1.145,

0.969 and 0.841 for Ni, Al, Ni<sub>3</sub>Al and Fe as modeled by EAM, respectively. For DFT/LDA-Si,  $\alpha$  for the glide set is determined to be 7.249. The  $\alpha$  for the shuffle set was determined to be  $-2.234$ . Such estimates give good results, within a few percent for  $G$  under pure mode I.

We accordingly give the procedure for a rudimentary estimate of the critical loading for dislocation emission from a crack tip:

- (A) Find the effective stress intensity factor for  $r$ - $\theta$ - $z$  coordinates, so as to find the  $K_r$  and  $K_\tau$  under general loading ( $K_I$ ,  $K_{II}$ ,  $K_{III}$ ), and then the phase angle  $\psi$ .
- (B) Find the tension reduced  $\gamma_{us}(\psi)$  according to (48).
- (C) Apply the calibrated equation for the critical condition, using the appropriate  $\eta$  coefficient.

$$K_r = \eta \sqrt{\gamma_{us} p(\theta, \phi)}. \quad (50)$$

This procedure gives an estimated error within the range  $\pm 7\%$  in  $G_d$  when applied to typical cases.

As can be seen in Table 2, the parameter  $\eta$  is of about the same value in different materials for each crack orientation and  $(\theta, \phi)$  angle. For example, regarding emission of the first Shockley partial in crack  $D$  ( $54.7^\circ$ ,  $60^\circ$ ),  $\eta$  is about 0.954; in crack  $E$  ( $54.7^\circ$ ,  $60^\circ$ ), it is 0.968 for II-Ni, III-Ni, Al, Ni<sub>3</sub>Al and Si (glide set).

### Conclusion and summary

The meaning of the critical loading for dislocation emission from a crack tip given in Table 2 can be elucidated by comparison with available atomistic simulations of loaded crack tips of EAM-Fe (Cheung *et al.*, 1991) and EAM-Al (Hoagland *et al.*, 1990). The preliminary comparison was presented in Sun (1993). The critical loading for each crack orientation and material listed in Table 2 is compared with those based on the isotropic formulations in Table 4 of Sun *et al.* (1993). It is also useful to compare to the Griffith cleavage for crack extension when  $G_c = 2\gamma_s$ , so as to predict the intrinsic ductile versus brittle response.

For crack  $A$  in EAM-Fe, for which the usual slip system has  $\theta = 45^\circ$  and  $\phi = 35.3^\circ$  with respect to the crack tip, the anisotropic  $G$  is 2.4 times the isotropic one in the shear-only model; in the combined tension-shear model, even the instability is different in that the anisotropic model gives crack branching while the isotropic model gives dislocation emission. The two  $G$  values are similar, though. For crack  $B$ , the combined tension-shear  $G$  values for dislocation emission in the anisotropic formulation are 40% less than the isotropic equivalent; for crack  $C$ , the anisotropic  $G$  is 2.4 times the isotropic  $G$ . Therefore, the anisotropic formulation is essential for EAM  $\alpha$ -Fe.

For fcc materials, the  $G$  values in the two formulations are about 10–25% different, in both the shear-only and tension-shear coupled models.

To illustrate that the anisotropic formulation can be important even for the smaller differences, we present results for Ni<sub>3</sub>Al in two crack orientations under mode I loading. In the anisotropic formulation we use  $C_{11} = 2.516 \times 10^{11}$  Pa,  $C_{12} = 1.370 \times 10^{11}$  Pa and  $C_{44} = 1.262 \times 10^{11}$  Pa, which are the fitted elastic

moduli via the EAM functions. In the corresponding isotropic problem we use the Voigt averaged elastic moduli of the three elastic constants, namely,  $\mu = (C_{11} - C_{12} + 3C_{44})/5 = 0.9864 \times 10^{11}$  Pa,  $\lambda = (C_{11} + 4C_{12} - 2C_{44})/5 = 1.094 \times 10^{11}$  Pa, and the corresponding Poisson ratio  $\nu$  is 0.263.

For crack extension under pure mode I, the critical loading can be determined by the Griffith condition, i.e.  $G_c = \gamma_{s1} + \gamma_{s2}$ , for cleaving along a perfect crystal plane, where  $\gamma_{s1}$  and  $\gamma_{s2}$  are the surface energies of the two cleaved surfaces. Expressed in terms of the crack extension force, the cleavage condition is the same for both anisotropic and isotropic elasticity.

We treat the crack orientations  $D$  and  $E$  for  $\text{Ni}_3\text{Al}$ . For crack tip orientation  $D$  with the (001) crack plane, growing along  $[\bar{1}10]$ , with a [110] front, the slip plane is  $(\bar{1}\bar{1}1)$ , and the inclination angle  $\theta = 54.7^\circ$ . The first emitted Shockley partial would correspond to  $\phi = 60^\circ$ . In the shear-only model, the solution of the critical condition in the anisotropic formulation gives  $G_d/\gamma_{us} = 28.43$ . Using the isotropic formulation, the shear-only model gives  $G_d/\gamma_{us} = 22.79$ . Here, the isotropic approximation gives a 19.9% discrepancy.  $G_c$  for crack orientation  $D$  equals  $3.51 \text{ J m}^{-2}$ , while  $G_d$  is, using the relaxed value of  $0.315 \text{ J m}^{-2}$  for  $\gamma_{us}$ , equal to  $8.96 \text{ J m}^{-2}$  with the anisotropic treatment. Because  $G_d$  is much larger than  $G_c$ , the (001) cracks are brittle. The isotropic treatment gives a  $G_d$  equal to  $7.18 \text{ J m}^{-2}$ , and thus predicts that the (001) cracks are brittle.

In the tension–shear coupled model, the critical condition for dislocation emission from crack  $D$  in the anisotropic formulation is that  $G_d = 5.59 \text{ J m}^{-2}$  with the constitutive law for the first Shockley partial slip as determined in Sun *et al.* (1993) for  $\text{Ni}_3\text{Al}$ . Hence, crack  $D$  is predicted to be brittle against emission of the first Shockley partial. In the isotropic formulation,  $G_d = 5.77 \text{ J m}^{-2}$ , which is greater than  $G_c$ . Hence, the isotropic formulation gives a 3.2% discrepancy from the anisotropic, and also predicts that {001} cracks growing along  $\langle 110 \rangle$  are in a brittle crack orientation. The  $G_d$  values cited are close enough to  $G_c$  that thermal activation would be an important factor, allowing nucleation when  $G_d \approx G_c$ .

Crack tip orientation  $E$ , with a  $(\bar{1}10)$  crack plane, growing along [001], with a [110] front, is associated with the  $(\bar{1}\bar{1}1)$  slip plane, hence the inclination angle  $\theta$  is  $35.3^\circ$ . The first Shockley partial that is emitted would correspond to  $\phi = 0^\circ$  here. In the shear-only model, anisotropic formulation, the solution of the critical condition gives the  $G_d/\gamma_{us} = 10.39$ , so  $G_d$  is  $3.27 \text{ J m}^{-2}$ . For crack  $E$  to extend, the  $G_c$  is  $3.65 \text{ J m}^{-2}$ . Because  $G_d$  is lower than  $G_c$ , the {110} cracks growing along  $\langle 001 \rangle$  are ductile. However, using the isotropic formulation,  $G_d/\gamma_{us} = 12.21$ , which means that  $G_d$  is  $3.85 \text{ J m}^{-2}$  and is greater than  $G_c$  for cleavage. Here, the isotropic formulation not only gives a 17.5% discrepancy with the anisotropic but also predicts that crack  $E$  is brittle, which is contrary to the anisotropic prediction.

To differentiate the similar critical loading conditions for dislocation emission and cleavage in this case, the results of the tension–shear coupled model are also presented. In the anisotropic formulation,  $G_d = 2.60 \text{ J m}^{-2}$  with the tension–shear coupled law for the first Shockley partial slip; hence, crack  $E$  is predicted to be ductile for emission of the first Shockley partial. The isotropic formulation gives  $G_d = 3.025 \text{ J m}^{-2}$ , which is less than  $G_c$ . Here, the isotropic formulation gives a 16.3% discrepancy, and also predicts that {110} cracks growing along  $\langle 001 \rangle$  are ductile.

As we might expect to be the general trend, the bcc structure is more anisotropic than the fcc structure (including Ni, Al, Ni<sub>3</sub>Al and Si). The difference in the critical  $G$  between isotropic and anisotropic formulations for bcc materials is larger than in fcc materials. Such differences should correlate with the anisotropic factors of these materials,  $2C_{44}/(C_{11} - C_{12})$ , which are 7.00 for Fe, 3.24, 3.01 and 2.20 for Ni, Al and Ni<sub>3</sub>Al, respectively, and 1.56 for Si (the smallest of these materials).

In the tension–shear model, the two formulations may present different instability modes of either dislocation nucleation or crack branching, as described above for EAM  $\alpha$ -Fe. The anisotropic  $G$  values may be less or greater than the isotropic correspondents. For EAM  $\alpha$ -Fe, the anisotropic formulation results are 2.4 times the isotropic ones in crack  $C$ , and similar for the effective approximation model, the shear-only and tension–shear coupled model; in crack  $A$ , the anisotropic formulation values are again 2.4 times the isotropic ones in the effective approximate model and shear-only model. However, in crack  $B$ , the anisotropic formulation results are 40% less than the isotropic ones, similarly in the effective approximation model, the shear-only and tension–shear coupled model. In the fcc lattices, Ni, Al and Ni<sub>3</sub>Al, we conclude that the two formulations give results with a difference in the range of  $\pm 10$ –25%. For DFT-LDA-Si, both the glide and shuffle slip systems, the two formulations are very similar; the difference in the critical  $G$  is less than 14%. In the tension–shear coupled model, the two formulations give the same instability for dislocation emission or crack branching, and the difference is less than 4%. We may conclude that for Si, the isotropic formulation is a good approximation. It would consequently support the use of the isotropic formulation in the analysis of activation energy for dislocation emission in Si by Rice and Beltz (1994) and Beltz and Rice (1994).

As mentioned previously, the validity of the Peierls model can be limited by several phenomena. Recent atomic studies by Zhou *et al.* (1994) showed that the critical loading for dislocation emission can be quite different from the predicted values by the Peierls model in the tilted slip plane case. A possible cause of the discrepancy is due to the discrete nature of the system, resulting in lattice trapping or the ledge effect. The atomistic simulations by Becquart *et al.* (1993) show that the surface reconstruction of near-tip crack surfaces is an important factor influencing the condition for dislocation emission. These are open questions for further research.

## COUPLING BETWEEN IN-PLANE AND ANTI-PLANE ELASTICITY

So far, we assumed that the  $z$  axis along the crack front is perpendicular to a mirror plane for the lattice, so that the in-plane field quantities are decoupled from the anti-plane ones. If this were not true, the assumption is only good as an approximation. For the exact method of treatment for the coupled case, see Stroh (1958), Barnett and Asaro (1972) and Suo (1989).

## ACKNOWLEDGEMENTS

We would like to thank J. R. Rice for his guidance, encouragement and critical comments during this project. Discussions with J. W. Hutchinson and D. M. Stump and help of D. Galpin

on preparing the manuscript are also acknowledged. This work was supported by the Office of Naval Research, Mechanics Division (grants N00014-90-J-1379 and N00014-92-J-1960). Some of the computations were carried out under NSF support at the Pittsburgh Supercomputing Center. G.E.B. also acknowledges support of a postdoctoral appointment with the Solid Mechanics group at Brown University, as well as a fellowship from the Alexander von Humboldt Foundation (at the Max-Planck-Institut für Metallforschung, Institut für Werkstoffwissenschaft, Stuttgart), during the final stages of this work.

## REFERENCES

- Asaro, R. J. (1975) An image force theorem for a dislocation near a crack in an anisotropic elastic medium. *J. Phys. F: Metal Phys.* **5**, 2249–2255.
- Atkinson, C. (1966) The interaction between a dislocation and a crack. *Int. J. Fracture Mech.* **2**, 567–575.
- Barnett, D. M. and Asaro, R. J. (1972) The fracture mechanics of slit-like cracks in anisotropic media. *J. Mech. Phys. Solids* **20**, 353–366.
- Barnett, D. M. and Lothe, J. (1974) An image force theorem for dislocations in anisotropic bicrystals. *J. Phys. F: Metal Phys.* **4**, 1618–1635.
- Becquart, C. S., Clapp, P. C. and Rifkin, J. A. (1993) Molecular dynamics simulation of fracture in RuAl. *High-Temperature Ordered Intermetallic Alloys V* (ed. I. Baker, R. Darolia, J. D. Whittenberger and M. H. Yoo), MRS Symp. Proc., Vol. 288, pp. 519–524.
- Beltz, G. E. (1992) The mechanics of dislocation nucleation at a crack tip. Ph. D. thesis, Div. of Applied Sciences, Harvard University, Cambridge, MA.
- Beltz, G. E. and Rice, J. R. (1991) Dislocation nucleation versus cleavage decohesion at crack tips. *Modeling the Deformation of Crystalline Solids* (ed. T. C. Lowe, A. D. Rollett, P. S. Follansbee and G. S. Daehn), TMS, pp. 457–480.
- Beltz, G. E. and Rice, J. R. (1994) The activation energy for dislocation nucleation in silicon. In preparation.
- Bilby, B. A. and Eshelby, J. D. (1968) Dislocations and the theory of fracture. *Fracture: An Advanced Treatise* (ed. H. Liebowitz), Vol. 1, pp. 99–182. Academic Press, New York.
- Cheung, K. S. (1990) Atomistic study of dislocation nucleation at a crack tip. Ph.D. Thesis, Dept. of Nuclear Engineering, MIT, Cambridge, MA.
- Cheung, K. S., Argon, A. S. and Yip, S. (1991) Activation analysis of dislocation nucleation from a crack tip in  $\alpha$ -Fe. *J. Appl. Phys.* **69**(4), 2088–2096.
- Cheung, K. S. and Yip, S. (1990) Brittle–ductile transition in intrinsic fracture behavior of crystals. *Phys. Rev. Lett.* **65**(22), 2804–2807.
- Cheung, K. S. and Yip, S. (1994) Molecular dynamics simulation of crack tip extension: brittle to ductile transition. *Modelling and Simulation in Materials Science and Engineering* (in press).
- Duesbery, M. S., Michel, D. J., Kaxiras, E. and Joos, B. (1990) Molecular dynamics studies of defects in Si. *Defects in Materials* (ed. P. D. Bristowe, J. E. Epperson, J. E. Griffith and Z. Liliental-Weber), MRS Symp. Proc., Vol. 209, pp. 125–130.
- Erdogan, F. (1975) Complex function technique. *Continuum Physics* (ed. A. C. Eringen), pp. 523–603. Academic Press, New York.
- Erdogan, F. and Gupta, G. D. (1972) On the numerical solution of singular integral equations. *Quart. Appl. Math.* **29**, 525–534.
- Foiles, S. M., Baskes, M. I. and Daw, M. S. (1986) Embedded-atom-method functions for the fcc metals Cu, Ag, Au, Ni, Pd, Pt, and their alloys. *Phys. Rev. B* **33**, 7983–7991.
- Foiles, S. M. and Daw, M. S. (1987) Application of the embedded atom method to Ni<sub>3</sub>Al. *J. Mater. Res.* **2**(1), 5–15.
- Harrison, R. J., Spaepen, F., Voter, A. F. and Chen, A. F. (1990) Structure of grain boundaries in iron. *Innovations in Ultrahigh-Strength Steel Technology* (ed. G. B. Olson, M. Azrin and E. S. Wright), pp. 651–675. Plenum Press, New York.

- Hirth, J. P. and Lothe, J. (1982) *Theory of Dislocations*, 2nd edn. McGraw-Hill, New York.
- Hoagland, R. G., Daw, M. S., Foiles, S. M. and Baskes, M. I. (1990) An atomic model of crack tip deformation in aluminum using an embedded atom potential. *J. Mater. Res.* **5**, 313–324.
- Huang, Y. M., Spence, J. C. H., Sankey, O. T. and Adams, G. B. (1991) The influence of internal surfaces on the  $(2 \times 1)$  shuffle and glide cleavage reconstructions for Si (111). *Surface Sci.* **256**, 344–353.
- Kaxiras, E. and Duesbery, M. S. (1993) Free energies of generalized stacking faults in Si and implications for the brittle–ductile transition. *Phys. Rev. Lett.* **70**(24), 3752–3755.
- Nabarro, F. R. N. (1947) Dislocations in a simple cubic lattice. *Proc. Phys. Soc.* **59**, 256–272.
- Peierls, R. E. (1940) The size of a dislocation. *Proc. Phys. Soc.* **52**, 34–37.
- Rice, J. R. (1968a) A path independent integral and the approximate analysis of strain concentration by notches and cracks. *J. Appl. Mech.* **35**, 379–386.
- Rice, J. R. (1968b) Mathematical analysis in the mechanics of fracture. *Fracture: An Advanced Treatise*, Vol. 2, *Mathematical Fundamentals* (ed. H. Liebowitz), Ch. 3, pp. 191–311. Academic Press, New York.
- Rice, J. R. (1985) Conserved integrals and energetic forces. *Fundamentals of Deformation and Fracture, Eshelby Memorial Symposium* (ed. B. A. Bilby, K. J. Miller and J. R. Willis), pp. 1–56. Cambridge University Press.
- Rice, J. R. (1992) Dislocation nucleation from a crack tip: an analysis based on the Peierls concept. *J. Mech. Phys. Solids* **40**, 239–271.
- Rice, J. R. and Beltz, G. E. (1994) The activation energy for dislocation nucleation at a crack. *J. Mech. Phys. Solids* **42**, 333–360.
- Rice, J. R., Beltz, G. E. and Sun, Y. (1992) Peierls framework for dislocation nucleation from a crack tip. *Topics in Fracture and Fatigue* (ed. A. S. Argon), pp. 1–58. Springer, Berlin.
- Rice, J. R. and Thomson, R. (1974) Ductile vs. brittle behavior of crystals. *Phil. Mag.* **29**, 73–97.
- Schöck, G. (1991) Dislocation emission from crack tips. *Phil. Mag.* **A63**, 111–120.
- Stroh, A. N. (1958) Dislocations and cracks in anisotropic elasticity. *Phil. Mag.* **3**, 625–646.
- Sun, Y. (1993) Atomistic aspects of dislocation/crack tip interaction. Ph.D. thesis, Div. of Applied Sciences, Harvard University, Cambridge, MA.
- Sun, Y., Beltz, G. E. and Rice, J. R. (1993) Estimates from atomic models of tension–shear coupling in dislocation nucleation from a crack tip. *Mater. Sci. Engng* **A170**, 67–85.
- Sun, Y., Rice, J. R. and Truskinovsky, L. (1991) Dislocation nucleation versus cleavage in  $\text{Ni}_3\text{Al}$  and Ni. *High-Temperature Ordered Intermetallic Alloys IV* (ed. L. A. Johnson, D. T. Pope and J. O. Stiegler), MRS Symp. Proc., Vol. 213, pp. 243–248.
- Suo, Z. (1989) Singularities interacting with interfaces and cracks. *Int. J. Solids Struct.* **25**(10), 1133–1142.
- Suo, Z. (1990) Singularities, interfaces and cracks in dissimilar anisotropic media. *Proc. R. Soc. Lond.* **A427**, 331–358.
- Zhou, S. J., Carlsson, A. E. and Thomson, R. (1993) Dislocation nucleation and crack stability: lattice Green's-function treatment of cracks in a model hexagonal lattice. *Phys. Rev. B* **47**(13), 7710–7719.
- Zhou, S. J., Carlsson, A. E. and Thomson, R. (1994) Crack blunting effects on dislocation emission from cracks. *Phys. Rev. Lett.* **72**(6), 852–855.

## APPENDIX: DISLOCATION AND CRACK TIP INTERACTIONS IN AN ANISOTROPIC ELASTIC MEDIUM

The functions  $F_{\alpha\beta}(r, s, \theta)$  and  $g_{\alpha\beta}(r, s, \theta)$  are required for treating the problem of a dislocation interacting with a crack. The stress distribution around the tip in an anisotropic medium without a dislocation and with one has been solved, originally by Stroh (1958), Atkinson (1966), Barnett and Asaro (1972), Asaro (1975) and summarized by Suo (1989) using the stress

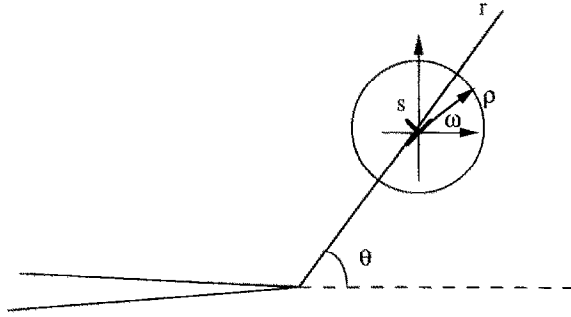


Fig. A1. A dislocation interacting with crack tip in an anisotropic medium.

function method. Here, we prove two elegant theorems regarding the functions  $g_{\alpha\beta}(r, s, \theta)$ . The scenario is illustrated in Fig. A1. Suppose a dislocation of Burgers vector  $b_\beta$  is located at  $(s, \theta)$  in a polar coordinate system from the crack tip. The local polar coordinate system at the dislocation core is  $(\rho, \omega)$ .

Near the dislocation, the stress  $\sigma_{ij}(\rho, \omega)$  behaves like  $1/\rho$ . From Rice (1985), we deduce that

$$h_k(\omega)\sigma_{ki}(\rho, \omega) = \frac{1}{4\pi} \frac{\Lambda_{ij}^{-1} b_j}{\rho}, \quad \text{when } \rho \text{ is small,} \tag{A1}$$

where  $h_i(\omega)$  is the unit vector in the direction of increasing  $\omega$ . Note that the right hand side of (A1) is independent of  $\omega$ , which results from the equation of force equilibrium. We can transform vectors and tensors in (A1) from an  $(x, y, z)$  coordinate system denoted in Latin indices to  $(r, \theta, z)$  denoted in Greek indices  $\alpha$  and  $\beta$  by a tensor transformation, by a rotation of angle  $\theta$  around the  $z$  axis. Further, setting  $\omega$  equal to  $\theta$ , we obtain

$$\sigma_{\theta\alpha}(\rho, \theta) = \frac{1}{4\pi} \frac{\Lambda_{\alpha\beta}^{(\theta)-1} b_\beta}{\rho} \tag{A2}$$

when  $\rho$  is small.

From the Atkinson (1966) solution and Suo (1989) treatment of a dislocation interacting with a crack tip in an anisotropic medium, we can show that when the dislocation lies in front of the crack tip on the crack plane, i.e.  $\theta = 0$ , the stress  $\sigma_{21}(r)$  ahead of the crack tip and in the plane is

$$\sigma_{21}(r) = \frac{1}{4\pi} \sqrt{\frac{s}{r}} \frac{\Lambda_{ij}^{-1} b_j}{r-s}. \tag{A3}$$

From (52) we can deduce that the stress intensity factors induced by the dislocation are

$$K_i = -\frac{1}{2\sqrt{2\pi s}} \Lambda_{ij}^{-1} b_j, \tag{A4}$$

where  $i = 1, 2$  and  $3$  for mode II, I and III, which was given by Rice (1985). We also observe that (A3) satisfies (A2).

For a dislocation lying on the inclined slip plane as shown in Fig. A1, we write the generalization of (A3) as

$$\sigma_{\theta\alpha}(r, \theta) \equiv g_{\alpha\beta}(r, s; \theta) b_\beta = \frac{1}{4\pi} \sqrt{\frac{s}{r}} \frac{[\Lambda_{\alpha\beta}^{(\theta)-1} + h_{\alpha\beta}(r/s, \theta)] b_\beta}{r-s}. \tag{A5}$$

In order to satisfy (A2) when  $\rho = r - s$  is small, we demand that

$$h_{\alpha\beta}(t = 1, \theta) = 0, \quad (\text{A6})$$

in order to have proper stress fields in the linear elastic medium near the dislocation point  $s$ . Furthermore, the Rice–Thomson image force theorem (1974), which was generalized by Asaro (1975) to anisotropic elasticity, and further generalized by Rice (1985) to the sector-wise different anisotropic elasticities at a crack tip, for a dislocation line at a crack tip implies that

$$\partial h_{\alpha\beta}(t = 1, \theta)/\partial t \text{ is antisymmetrical for indices } \alpha \text{ and } \beta. \quad (\text{A7})$$

Equation (A7) is proven next. We point out that (A6) and (A7) are generalizations from isotropic results deduced by Rice (private communication).

From Rice (1985), the attraction force received by the dislocation should be

$$f_r = -\frac{b_i \Lambda_{ij}^{-1} b_j}{8\pi s} = -\frac{b_\alpha \Lambda_{\alpha\beta}^{(ij)-1} b_\beta}{8\pi s}. \quad (\text{A8})$$

We can obtain the image force  $f_r$  by the following procedure. Consider the stress field of (A5) and decompose it into the field of a dislocation in an uncracked crystal, plus another term which is bounded at the dislocation. That other term, evaluated at  $r = s$  and multiplied by  $b_\alpha$ , gives the Peach–Köhler force, which must be consistent with (A8). Thus we establish that

$$b_\alpha \partial h_{\alpha\beta}(t = 1, \theta)/\partial t b_\beta = 0, \quad (\text{A9})$$

which is equivalent to (A7). We have omitted the details.